Plasma Modification of Solid and Porous Polyethylene

Scott G. Walton,* Evgeniya H. Lock,[a] Richard F. Fernsler

The use of electron beam generated plasmas to modify the surface of solid and porous polyethylene substrates is discussed. In both cases, the hydrophobicity of the material was increased by exposing the substrates to electron beam generated plasmas produced in Ar/SF_6 mixtures. The solid material studies served as a basis for understanding the plasma-induced changes at the substrate surface, while the porous material was treated using a system designed for two-sided processing applications and proved to be the best way to maximize treatment. Plasma diagnostics were used to characterize the ion and neutral fluxes at the substrates and thereby obtain a better understanding of the plasma–polymer interaction.

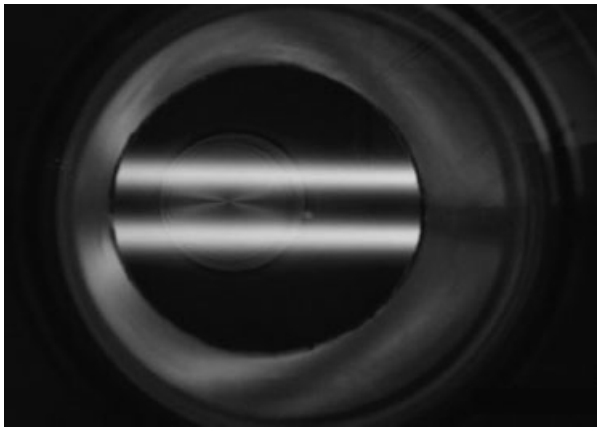

Introduction

Polymers are ubiquitous in the production of new materials and devices ranging from biomaterials[1] to organic[2] and flexible[3] electronics. While the bulk characteristics of polymers make them ideally suited for these and other applications, their surface characteristics are often not well suited for integration into devices. Thus, the polymer surface must be modified or functionalized prior to being used. Plasma-based techniques are particularly useful in altering the surface characteristics without affecting the bulk properties and have a number of advantages over wet processing, including low pollution and waste products, uniform treatment over nanoscale surface features, and processing at room-temperature operation. Plasma-produced energetic ions and reactive species are known to produce chemically active sites on the polymer surface that can lead to the desired functionality. Indeed, plasmas have been used to improve adhesion,[4] wettability,[5] hydrophobicity,[5] and biocompatibility.[6] There are, however, serious concerns over the delivery of energetic ions to the surface, since these ions can strongly alter the surface morphology or worse, damage the polymers.[7]

The Naval Research Laboratory has developed a materials processing system based on electron beam-generated plasmas for use in a range of applications.[8,9] When high-energy (≈2 keV) electron beams are used as the primary ionization source, the resultant plasmas have several unique characteristics when compared to conventional, low-pressure plasma sources. Since plasma production is confined to the electron beam volume, chamber, and source geometry can be readily modified to suit the processing application. Moreover, the ion flux at the substrate surface can be regulated by moving the substrate position with respect to the electron beam.[10] Also, species production at high electron energy is nearly directly proportional to the background gas concentrations.[10] Lastly and importantly for the processing of soft materials, the electron temperature is inherently low in these plasmas, which provides a small plasma potential and thus low

S. G. Walton, E. H. Lock, R. F. Fernsler
Plasma Physics Division, U.S. Naval Research Laboratory, 4555 Overlook Ave., SW, Washington, DC 20375, USA
Fax: (+1) 202 763 7531; E-mail: scott.walton@nrl.navy.mil

[a] NRL/NRC Postdoctoral Research Associate.

© 2008 WILEY-VCH Verlag GmbH & Co. KGaA, Weinheim
DOI: 10.1002/ppap.200800003

Early View Publication; these are NOT the final page numbers, use DOI for citation !!

energy of ions as they leave the plasma. In molecular gases, those temperatures are typically below 0.5 eV.[10]

The direct control over the intensity of the ion flux and the low incident ion energy provide a unique opportunity to study polymer modification using a controllable flux of ions whose kinetic energies are close to the binding energies of the species that make up the polymer chain constituents. Thus, excessive etching or worse, surface damage may be avoided. Electron beam-generated plasmas have already been used to change the functionality and surface chemistry of polymers,[4] while it was also shown that these plasmas produce less roughness in photoresists[11] than treatments by conventional discharges.[12]

In this work, we focus on the modification of solid and porous polyethylene (PE). The solid PE studies served as a basis for understanding PE interaction with electron beam generated plasmas. The porous PE was treated using a system designed for two-sided processing applications (e.g., the front and back of substrates). In both cases, the focus was on reducing the surface energy and thus increasing the hydrophobicity. To this end, electron beam generated plasmas produced in Ar/SF_6 were used as a way of introducing fluorine to the surface. For the solid PE, the surface energy of both untreated and treated samples was determined using the method developed by Fox and Zisman.[13] For the porous PE, a wicking test was developed to determine the relative changes in contact angles. In both cases, the surface energy was found to be reduced. For the porous substrates, the hydrophobicity was highest when the substrate was identically exposed on both sides. In addition, we present the results of plasma diagnostics to determine the general characteristics of the plasma used in these treatments.

Experimental Part

System

The production of electron beam generated plasmas has been described in detail elsewhere.[14] The experimental apparatus is shown in Figure 1 with the two-beam plasma source.[8] The system vacuum was maintained by a 250 $l \cdot s^{-1}$ turbo pump, with a base pressure on the order of 10^{-7} Torr. The operating pressure was achieved by introducing high-purity gases through mass flow controllers and throttling the pumping speed using a manual gate valve. A set of external field coils provided an axial magnetic field that varied by no more than 5% over the region of interest.

Plasmas were generated by high-energy electron beams produced by driving the hollow cathode with a -2 kV for a duration of 1–2 ms at a duty factor of 20–40%. The emergent beam passed through a slot in a grounded anode and was then terminated at a second grounded anode located further downstream. The electron beam volume between the two anodes defines the ionization source volume, with the dimensions set by

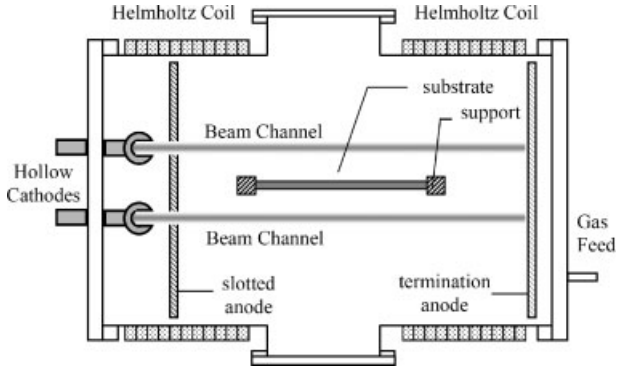

Figure 1. A schematic diagram of the processing system. The mass spectrometer is not shown in this schematic but is inserted from one of the side ports located perpendicular to the electron beam.

the slot size (1 cm × 10 cm) and the anode-to-anode length (40 cm). For the processing, one or both of the cathodes shown in Figure 1 were operated, depending on the desired process. The two slots are separated by 5 cm, giving a beam axis-to-beam axis distance of 6 cm. Beam spreading from collisions with the neutral background was largely eliminated using a co-axial magnetic field of 210 Gauss.

Surface Treatment

Two types of polymer materials were used for this work. The first was 1.6 mm thick solid high-density PE (McMaster-Carr) and the second was 0.06 mm thick PE filter material (Pall Corporation). The samples were suspended between the electron beams at the center of the system, which was approximately 3.0 cm from the axis of each beam. For the solid PE and when only one side of the PE filter material was treated, a stainless steel backing plate was placed behind the samples to add support and prevent direct plasma exposure. Prior to each treatment, the chamber was evacuated to a base pressure less than 10^{-6} Torr. After treatment, the chamber was evacuated to a pressure less than 10^{-5} Torr prior to removing the materials for post-treatment, ex situ surface diagnostics. For the solid PE treatments, a range of operating conditions was explored while keeping the total pressure constant at 60 mTorr. This included a variation in the period, duty factor, and gas background. For the porous PE materials, operating conditions were held constant.

In order to determine changes in the surface properties of the solid polymers, the method developed by Fox and Zisman[13] was used to estimate the critical surface tension, which is correlated to the surface energy, of both untreated and plasma-treated samples. For this method, the contact angles of the liquids were measured, and the cosines of those angles were plotted as a function of the liquid surface tension. The critical surface tension of the polymer can be estimated by extrapolating the data to $\cos\theta = 1$. The contact angle of various liquids was determined using a goniometer and the drop volume was approximately 2 μl. Table 1 shows the liquids used and their critical surface tensions. Since the liquids were not from the same homologous series (e.g., octane, dodecane,

© 2008 WILEY-VCH Verlag GmbH & Co. KGaA, Weinheim
DOI: 10.1002/ppap.200800003
↖ Early View Publication; these are NOT the final page numbers, use DOI for citation !!

Table 1. Liquids and their surface tensions used in the determination of critical surface tension.

Liquid	Surface tension
	dynes · cm^{-1}
Octane	22
Methanol	23
Dodecane	25
Hexadecane	28
1,4-Dioxane	33
Benzylalcohol	39
Ethylene glycol	48
Ammonium hydroxide	63
Water	73

and hexadecane), the data were extrapolated using the approach of Fowkes,[15] which employs an inverse square fit.

In order to test the change in the surface energy of the porous materials, a simple wicking test was developed. For this test, the porous PE was suspended in a small liquid reservoir of ethanol and covered, and the wicking height of the ethanol was measured as a function of time. To improve the height measurements, two small marks, separated by 1 cm, were placed on the material before submersion in the ethanol. Then, time-stamped photographs of the material were taken at various intervals, and the change in height with respect to the two marks was determined from those photographs. The error introduced using this technique is estimated to be less than 10%.

Plasma Diagnostics

Plasma diagnostics include ion flux and neutral density measurements, which were measured at the center of a grounded, 5.7 cm diameter stainless steel electrode using a Hiden EQP 300 Plasma Probe. Species enter the EQP through a 50 μm diameter aperture in the center of the electrode located 1.5 cm from the beam axis. Once inside, the ions are first energy selected by an electrostatic energy analyzer (EA) and then mass filtered by a quadrupole mass spectrometer (QMS). The EA was operated at a fixed resolution ($\Delta E/E_t$) with an uncertainty of approximately ±0.15 eV. For the ion flux measurements, data acquisition is time-resolved and the gating techniques have been described elsewhere.[16] For the neutral density measurements, an ionizer located after the entrance aperture generates ions, which are then detected as described above. The EQP has not been calibrated to determine the absolute flux of each species, so the intensity of the measured signal is reported in arbitrary units.

For these measurements, a single cathode was used, similar to that described in the previous work.[17] In addition, the magnetic field was turned off, since the high magnetic fields used in the processing work limited the transmission of ions through the EQP. With the exception of the magnetic field, all other operating conditions were the same as in the processing work. While the lack of a magnetic field will affect the ion flux, the difference is expected to be small and so these measurements relate well to the processing experiments.

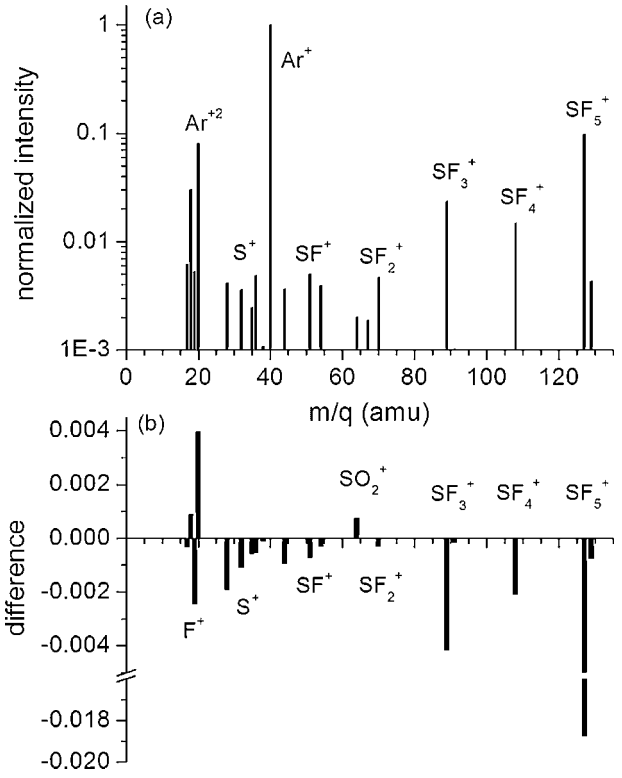

Figure 2. (a) The neutral density spectrum measured while the plasma is operating and (b) the difference spectrum comparing the neutral density spectrum while the plasma is running with the neutral density spectrum in the absence of plasma.

Results and Discussion

Plasma Diagnostics

Shown in Figure 2(a) is the neutral density spectrum (normalized to Argon) measured while the plasma is operating. For all mass spectra, data were acquired in increments of 0.1 amu and then the intensity at each mass was determined by summing the intensity across a width of ±0.4 amu. Shown in Figure 2(b) is a difference spectrum determined by subtracting the normalized neutral density spectrum while the plasma is off, from the normalized spectrum while the plasma is on. Since these measurements are time-averaged, the plasma-on and plasma-off measurements were taken over the same amount of time. The difference spectrum is indicative of the dissociation of the background gas. More specifically, the daughter species of SF_6 [F, S, and SF_n ($n = 1$–5)] decrease when the plasma is on, meaning there is less SF_6 present. The dissociation

© 2008 WILEY-VCH Verlag GmbH & Co. KGaA, Weinheim

Early View Publication; these are NOT the final page numbers, use DOI for citation !!

fraction could be determined from the difference spectrum[18] using the relative change in SF_5^+, in this case about 15%. Repeated measurements, however, show a large spread (5–15%), with the most common value being less than 10%. The reasons for this spread are unknown, although it likely results from a combination of system drift and measurement error. It is worth noting that for most gases, the ionization cross-section exceeds the dissociation cross-section at high electron impact energies, and so a dissociation fraction less than 10% is not unreasonable. We assume electron–ion recombination contributes to the production of radicals. However, the authors are not aware of any information regarding the rates of either direct or dissociative electron–ion recombination of SF_n^+ ions.

Shown in Figure 3(a) is the raw ion flux mass distribution measured at the electrode. Figure 3(b) shows the data after summing across the peaks as indicated above and normalizing to the intensity of the S^+ ion. The isotopes of the SF_n^+ ions associated with the sulfur isotopes (^{32}S, ^{33}S, and ^{34}S) were removed from the spectrum for clarity. Included in Figure 3(b) are the electron-impact ionization cross-sections for 1 keV electrons,[19] adjusted for the relative concentration of argon and SF_6, and then normalized to the S^+ cross-section. That is, the partial cross-sections were multiplied by 0.33 for SF_6 and 0.66 for Ar, and those values were then normalized to the adjusted S^+ partial cross-section. This provides a clear indication of ion losses within the system. Recall that ionization is localized to the beam volume and as ions diffuse toward the electrode face, charge exchange reactions with SF_6 will alter the relative densities as compared to what would be expected from ionization alone. S^+ was chosen as the normalization species since it is has one of the lowest ionization potentials and is thus unlikely to charge exchange with the background gas (SF^+ and SF_2^+ are also reasonable choices). The daughter ions of SF_6 (SF_n^+) exhibit intensities that are larger and the charge exchange reactions of note for this work include, along with their respective rate constants:

$$Ar^+ + SF_6 \rightarrow SF_5^+ + F + Ar;\ k{\sim}9.3\times10^{-10}cm^3\cdot s^{-1}\ [ref.^{[20]}]$$

$$SF_5^+ + SF_6 \rightarrow SF_3^+ + F_2 + SF_6;\ k{\sim}5.4\times10^{-12}cm^3\cdot s^{-1}\ [ref.^{[21]}]$$

$$SF_3^+ + SF_6 \rightarrow S_2F_7^+ + F_2;\ k{\sim}3\times10^{-13}cm^3\cdot s^{-1}\ [ref.^{[22]}].$$

Since the ionization potential of F (17.4 eV) is higher than that of Ar (15.8 eV), F^+ will also likely charge exchange with SF_6 to produce SF_5^+.

Shown in Figure 4 are Ar^+ and SF_5^+ ion energy distributions measured at a floating electrode (the floating electrode simulates the surface of the polymer). For these measurements, the operating pressure was 60 mTorr and the argon and SF_6 flows were 25 and 10 sccm, respectively. The ion energies shown in Figure 4 are plotted as a function of EA voltage rather than energy. The distribution extends to negative voltages because the EA is referenced to ground and the electrode is floating. We also note that in electronegative gases (SF_6 or O_2), it is not uncommon to have surface charging.[23] This, of course, makes it difficult to determine the true energy. Nonetheless, the estimated energy is indicated along the top axis and was determined by arbitrarily assuming the zero of the energy scale to occur at approximately 10% of the maximum intensity of the lowest measured ion signal, which is the Ar^+ ion. At these energies the ion flux is expected to do little damage to the PE surface.

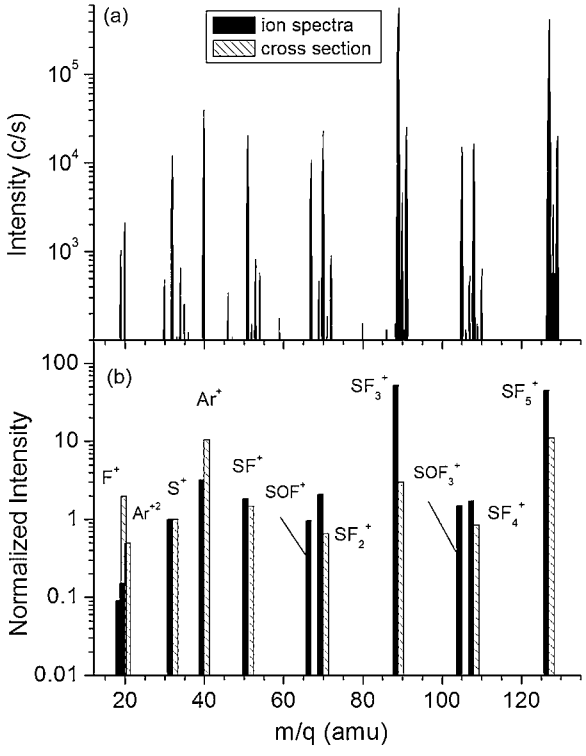

Figure 3. (a) The ion mass spectrum measured at an electrode located adjacent to plasmas produced in Ar/SF_6 mixtures and (b) the normalized spectrum and the normalized electron impact cross-sections from ref. [22] for 1 keV electrons.

Surface Treatment

For the solid PE treatments, a range of operating conditions was explored while keeping the total pressure constant at 60 mTorr. The plasma period (10 and 5 ms) and pulse width (1 and 2 ms) were varied to give duty factors between 20 and 40%. The total plasma exposure time, taken to be the plasma on time, was held constant at 4 min. The gas flows and gas background were also varied. The total gas flow was adjusted to give a high flow rate of 76 sccm (Ar/SF_6;

© 2008 WILEY-VCH Verlag GmbH & Co. KGaA, Weinheim
DOI: 10.1002/ppap.200800003
↖ Early View Publication; these are NOT the final page numbers, use DOI for citation !!

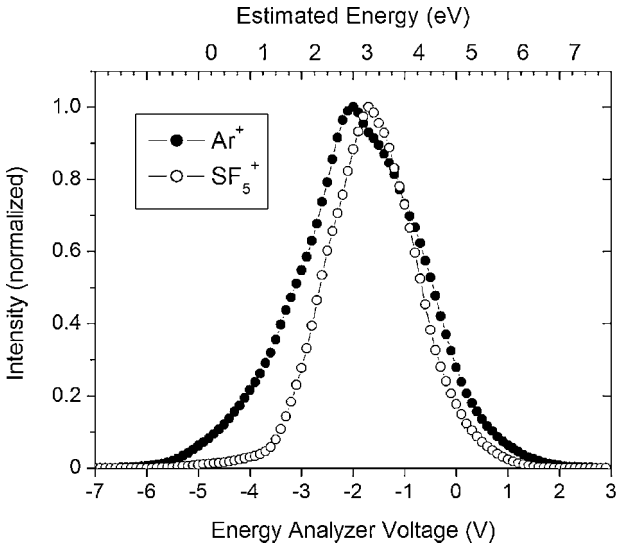

Figure 4. Ion energy distribution at surfaces located adjacent to plasmas produced in Ar/SF_6 mixtures.

60:16 sccm) and a low flow of 35 sccm (Ar/SF_6; 25:10 sccm). One of the treatments included a 2 min exposure to a pure argon plasma ($P = 38$ mTorr, 25 sccm) before the mixtures were introduced for the remaining 2 min. In addition, a treatment in pure argon only ($P = 60$ mTorr, 35 sccm) using a period of 10 ms (20% duty) and a total plasma exposure of 4 min was performed. The change in the critical surface tension of solid PE samples, following plasma treatment, is shown in Figure 5 and 6. To benchmark the importance of an ion flux, two tests were performed. In the first, the sample was exposed only to an Ar/SF_6 background with no plasma. In the second, the substrate was placed along the

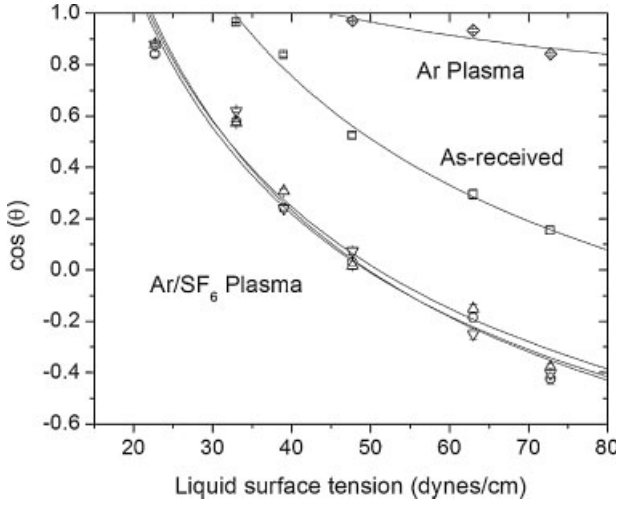

Figure 5. Zisman plot for untreated and plasma-treated solid PE. The critical surface tension is determined by extrapolating the data to cos $(\theta) = 1$.

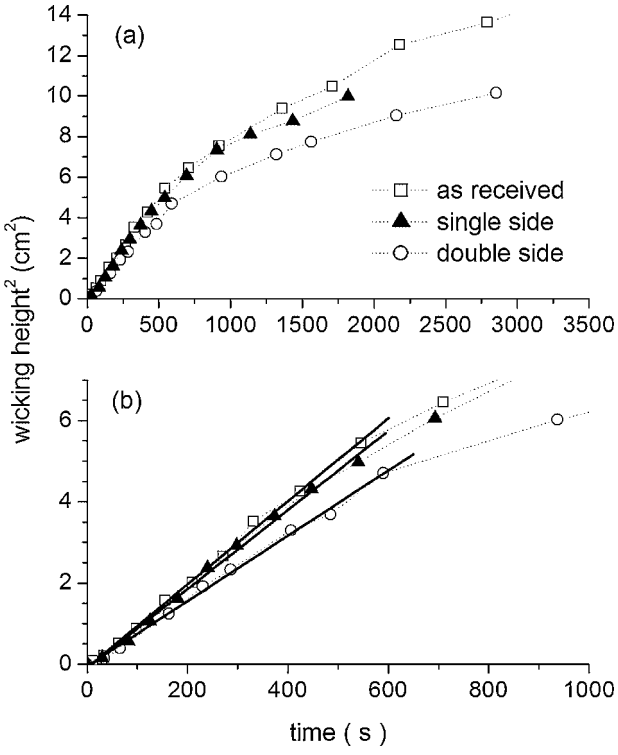

Figure 6. Ethanol wicking test for untreated and plasma treated porous PE.

reactor wall and thus subject to the neutral products without any significant ion flux. If the walls were not a significant neutral sink, which would require that the walls are saturated, then the reactive radical flux would be comparable to the flux at the stage. If however, the walls behave as a sink, then the reactive radical flux would be lower relative to the flux at the stage. For both of these samples, there was no change in the critical surface tension compared to the untreated samples. Thus, it is reasonable to assume, provided the reactive radical flux was not too low, that a flux of ions was required for surface modification.

Treating the samples in plasmas produced in Ar/SF_6 mixtures decreased the critical surface tension, which results in a more hydrophobic surface. The critical surface tension of PE was reduced by about 32%. Although not shown in this work, XPS measurements of PE treated using an electron beam produced plasma[4] have shown fluorine is incorporated into the polymer and the formation of CF_n functional groups are responsible for the increased hydrophobicity.[24] For plasma produced in pure argon, the critical surface tension was increased by approximately 40%, resulting in a more hydrophilic surface. Since argon is inert, this increase in critical surface tension is thought to be caused by oxygen incorporation when the sample was exposed to the atmosphere after treatment.[7]

© 2008 WILEY-VCH Verlag GmbH & Co. KGaA, Weinheim

Early View Publication; these are NOT the final page numbers, use DOI for citation !!

That is, the bombardment of the surface with argon ions is assumed to create active bonding sites that, when exposed to air, readily react with oxygen.

The critical surface tension shows no strong dependence on either the plasma duty or operating gas flow for the Ar/SF_6 plasma treatment. Changing the gas flow rate should only alter the reactive neutral species flux, thus again indicating the importance of ions. For a constant treatment time, changing the plasma duty factor varies the time during which ions are incident at the surface. If the changes in the critical surface tension were correlated only to ion-induced changes in morphology (e.g., sputtering and etching), those changes should increase with the duty factor. For the pure argon plasmas, on the other hand, the changes in surface tension suggest that ion-induced scissions of the polymer chain provide sites where oxygen can be incorporated. From these results, it is thus difficult to determine if the ion flux induces morphological changes or merely provides activate sites where fluorine or oxygen can be incorporated. However, it is apparent that ions are required to alter the surface energy based on the benchmark experiments where the samples were exposed only to the SF_6 containing background and when it was far from the ionization source.

Preliminary work showed the most effective way to increase the hydrophobicity of porous PE was to treat both surfaces of the material, as determined by an increase in the amount of time a drop of water took to be completely absorbed in the material. This was accomplished using a single beam system and first treating one side of the material, then turning the material over and treating the other side. This approach is, of course, time consuming and increases the chance of introducing contaminates.

The two beam system was developed to treat both sides of a material simultaneously. Since, as noted above, there appears to be no strong dependence on operating conditions, the process parameters for treating the porous PE were held constant at a total pressure of 60 mTorr, a total flow of 35 sccm (Ar/SF_6; 25:10 sccm), a period of 10 ms (20% duty), and total plasma exposure of 36 s.

The results of these studies are shown in Figure 6 and the differences between as-received, single-sided, and double-sided exposures are evident in the change in slope of the data sets. For a quantitative approach to understanding the differences, Lukas–Washburn[25] kinetics can be applied using the equation

$$h^2 = 0.5(r/\tau)(\gamma/\eta)(\cos\theta)t$$

where h is the wicking height, t the time, θ the contact angle, r the mean capillary radius, τ the surface tortuosity, γ the liquid surface tension, and η the liquid viscosity. This relationship holds only until gravitational effects and evaporation become important. At long wicking times, these effects slow the rise.[26] Since all terms for $h^2(\theta)$ are constants with the exception of the surface contact angle, it is evident from the change in slope after plasma treatment that the double-sided treatment has a greater effect on the contact angle and thus on the hydrophobicity of the porous PE. In order to estimate the change in contact angle, assume that the contact angle is zero for the untreated material (i.e., the ethanol is completely wetting). Next, solve for r/τ and assume it does not change with short plasma treatment times. Finally, solve for θ by using the slope of the plasma-treated data. After single- and double-sided treatments, the contact angles are approximately 18 and 38°, respectively.

These results provide only a limited understanding of the surface treatment but they indicate that the two-sided treatment is more effective at delivering reactive species and ions to both sides of the porous substrate. The most likely reactive species are fluorine and SF_n radicals, with the low-energy ion flux serving to enhance the incorporation of fluorine. The plasma density was not measured in these experiments, but from previous work,[27] the density was on the order of 10^{10}–10^{11} cm^{-3}. The Debye length is then 13 μm or more, based on an electron temperature of 0.5 eV. For pore diameters less than a micron wide (not an uncommon size), the sheath does not penetrate the pores and so ions do not penetrate as deeply as the neutrals, when the pore structure is at an angle with respect to the material surface and thus the sheath surface. This suggests that a direct comparison between the surface activation mechanism of solid and porous PE is only valid on the ion-exposed surfaces of the porous material, which would include both the outfacing material and line of sight material within the pores. Deep within the material, the changes at the surface would not be ion-activated, and based on the lack of changes in samples exposed to only the background gas and no ions, we can assume minimal changes. However, other authors have found changes on surfaces within porous materials, on areas that were not directly exposed to plasma.[28,29] From those works and ours, the treatment of porous materials will depend on pore size, material thickness, treatment type, and treatment time.

Conclusion

Experiments designed to investigate the treatment of polymers with electron beam-generated plasmas produced in mixtures of argon and SF_6 were performed. Plasma diagnostics showed that the incident ions have low energies and should not introduce any significant damage. It was also found that the background gas is weakly dissociated. The critical surface tension of solid PE was lowered when exposed to plasma produced in SF_6 mixtures, producing a surface that was more hydrophobic.

Plasma Process. Polym. **2008**, *5*, 000–000
© 2008 WILEY-VCH Verlag GmbH & Co. KGaA, Weinheim
DOI: 10.1002/ppap.200800003
↖ Early View Publication; these are NOT the final page numbers, use DOI for citation !!

These results were used to develop an approach for the treatment of porous PE filter material using a dual electron beam system. The hydrophobicity of porous PE was maximized when both sides of the material were exposed to plasma, compared to material exposed only on one side. These results suggest a flux of radicals and ions are required to maximize the modification of the material. Substrates of similar structure such as fabrics might also benefit from this simultaneous, two-sided approach to plasma treatment.

Acknowledgements: This work was supported by the *Office of Naval Research*. E. H. L. appreciates the support of the *National Research Council*.

Received: January 8, 2008; Revised: March 12, 2008; Accepted: March 19, 2008; DOI: 10.1002/ppap.200800003

Keywords: fluorination; ion-energy distribution functions (IEDF); plasma treatment; polyethylene (PE); polymer modification

[1] F. C. Simmel, W. U. Dittmer, D. N. A. nanodevices, *Small* **2005**, *1*, 284.
[2] M. J. Deen, M. H. Kazemeini, *Proc. IEEE* **2005**, *93*, 1306.
[3] R. S. Tarighat, A. Goodarzi, S. Mohajerzadeh, B. Arvan, M. R. Gaderi, M. Fathipour, *Proc. IEEE* **2005**, *93*, 1374.
[4] D. Leonhardt, C. Muratore, S. G. Walton, *IEEE Trans. Plasma Sci.* **2005**, *33*, 783.
[5] D. Hegemann, H. Brunner, C. Oher, *Nuclear Instrum. Methods Phys. Res. B* **2003**, *208*, 281.
[6] M. Garrison, R. Luginbel, R. Overney, B. Ratner, *Thin Solid Films* **1999**, *352*, 13.
[7] S. Tajima, K. Komvopoulos, *J. Phys. Chem. B* **2005**, *109*, 17623.
[8] D. Leonhardt, C. Muratore, S. G. Walton, R. A. Meger, *Surf. Coat. Technol.* **2004**, *188–189*, 299.
[9] D. Leonhardt, S. G. Walton, R. F. Fernsler, *Phys. Plasmas* **2007**, *14*, 057103.
[10] S. G. Walton, C. Muratore, D. Leonhardt, R. F. Fernsler, D. D. Blackwell, R. A. Meger, *Surf. Coat. Technol.* **2004**, *186*, 40.
[11] B. J. Orf, S. G. Walton, D. Leonhardt, G. S. Oehrlein, *J. Vac. Sci. Technol. A* **2007**, *25*, 779.
[12] S. Englemann, R. L. Bruce, T. Kwon, R. Phaneuf, G. S. Oehrlein, Y. C. Bae, C. Andes, D. Graves, D. Nest, E. A. Hudson, P. Lazzeri, E. Lacob, M. Anderle, *J. Vac. Sci. Technol. B* **2007**, *25*, 1353.
[13] H. W. Fox, W. A. Zisman, *J. Coll. Sci.* **1950**, *5*, 514.
[14] D. Leonhardt, S. G. Walton, C. Muratore, F. Fernsler, R. A. Meger, *J. Vac. Sci. Technol. A* **2004**, *22*, 2276.
[15] F. M. Fowkes, *Ind. Eng. Chem.* **1964**, *56*, 40.
[16] S. G. Walton, D. Leonhardt, R. F. Fernsler, *IEEE Trans. Plasma Sci.* **2005**, *33*, 838.
[17] S. G. Walton, D. Leonhardt, D. D. Blackwell, R. F. Fernsler, D. P. Murphy, R. A. Meger, *J. Vac. Sci. Technol. A* **2001**, *19*, 1935.
[18] Y. Wang, R. J. Van Brunt, J. K. Olthoff, *J. Appl. Phys.* **1998**, *83*, 703.
[19] R. Rejoub, D. R. Sieglaff, B. G. Lindsay, R. F. Stebbings, *J. Phys. B: At. Mol. Opt. Phys.* **2001**, *34*, 1289.
[20] Y. Ikezoe, S. Matsuoka, M. Takebe, A. Viggiano, *"Gas Phase Ion-Molecule Reaction Rates Through 1986"*, Ion Reaction Research Group of The Mass Spectroscopy Society of Japan, Distributed by Maruzen Co., Ltd., Tokyo, Japan 1989.
[21] K. Bederski, L. Wojcik, *Int. J. Mass Spectrom. Ion Proc.* **1996**, *154*, 145.
[22] Z. A. Talib, M. Saporoschenko, *Int. J. Mass Spectrom. Ion Proc.* **1992**, *116*, 1.
[23] J. K. Olthoff, R. J. Van Brunt, S. B. Radovanov, *Appl. Phys. Lett* **1995**, *67*, 473.
[24] S. M. Mukhopadhyay, P. Joshi, S. data, J. G. Zhao, P. France, *J. Phys. D: Appl. Phys.* **2002**, *35*, 1927.
[25] [25a] R. Lukas, *Kolloidn Zh.* **1918**, *23*, 15; [25b] E. W. Washburn, *Phys. Rev.* **1921**, *17*, 374.
[26] I. Pezron, G. Bourgain, D. Quere, *J. Colloid Interface Sci.* **1995**, *173*, 319.
[27] D. Leonhardt, S. G. Walton, D. D. Blackwell, W. E. Amatucci, D. P. Murphy, R. F. Fernsler, R. A. Meger, *J. Vac. Sci. Technol. A* **2001**, *19*, 136.
[28] C. X. Wang, Y. Ren, Y. P. Qiu, *Surf. Coat. Technol.* **2007**, *202*, 77.
[29] S. M. Mukhopadhyay, P. Joshi, S. Datta, J. G. Zhao, P. France, *J. Phys. D: Appl Phys.* **2002**, *35*, 1927.

© 2008 WILEY-VCH Verlag GmbH & Co. KGaA, Weinheim

Early View Publication; these are NOT the final page numbers, use DOI for citation !!